

New Results from the MINOS Experiment

Anna HOLIN^{*†}

University College London

E-mail: annah@hep.ucl.ac.uk

The MINOS experiment is a long-baseline neutrino experiment designed to study neutrino behaviour, in particular the phenomenon of neutrino oscillations. MINOS sends the NuMI neutrino beam through two detectors, a Near Detector 1 km downstream from the beam source at Fermilab, and a Far Detector 735 km away in the Soudan Mine in Minnesota. MINOS has been taking beam data since 2005. This document summarises recent neutrino oscillations results, with particular emphasis on electron neutrino appearance, which probes the angle θ_{13} of the neutrino mass mixing matrix. For an exposure of 8.2×10^{20} protons on target, MINOS finds that $\sin^2(2\theta_{13}) < 0.12$ for the normal mass hierarchy, and < 0.20 for the inverted mass hierarchy at the 90% C.L., if the CP-violating phase $\delta = 0$.

*XXIst International Europhysics Conference on High Energy Physics
21-27 July 2011
Grenoble, Rhones Alpes France*

^{*}Speaker.

[†]On behalf of the MINOS Collaboration

1. Neutrino Oscillations

In the past 20 years, one of the most significant developments in particle physics was the discovery of neutrino oscillations [1]-[6], indicating that neutrinos have mass. There are three generations (flavours) of neutrino, the electron, muon, and tau neutrino (ν_e, ν_μ, ν_τ). Each neutrino also has a corresponding anti-particle. Neutrino oscillations are parametrised using two mass squared differences (Δm_{21}^2 - solar sector, and Δm_{32}^2 - atmospheric sector), three mixing angles (θ_{12} , θ_{13} , and θ_{23}), and a CP violating phase (δ).

2. The MINOS Experiment

The MINOS experiment [7] is designed to probe neutrino behaviour and the phenomenon of neutrino oscillations by sending the NuMI neutrino beam through two detectors [8], the Near Detector at Fermilab, 1km downstream of the beam source, and the Far Detector in the Soudan Mine in Minnesota, 735km away. Both detectors are magnetized iron scintillator tracking calorimeters and are designed to be functionally identical to allow cancellation of certain systematic errors, like for example any mismodelling of the neutrino flux or cross-section. The NuMI neutrino beam is created by impacting 120 GeV protons onto a thin graphite target. The resulting hadrons (mostly pions and kaons) are collimated by two magnetic horns and then decay producing a beam of mostly ν_μ with a small 7% component of $\bar{\nu}_\mu$, and a 1.3% contamination of beam ν_e and $\bar{\nu}_e$. It is possible to reverse the horn current so as to achieve a beam with a higher proportion of muon antineutrinos.

3. Muon Neutrino Disappearance

MINOS oscillation analyses use the Near Detector to measure the neutrino interaction rate before any oscillations have occurred. These measured data are then extrapolated to the Far Detector to predict what would be seen in the absence of neutrino oscillations. This final data set is then unblinded and compared to the prediction. In the case of the ν_μ disappearance analysis, the survival probability of a muon neutrino is given by:

$$P(\nu_\mu \rightarrow \nu_\mu) \approx 1 - \sin^2(2\theta_{23}) \sin^2(1.27\Delta m_{32}^2(L/E)) \quad (3.1)$$

Figure 1 shows the results of the ν_μ disappearance analysis for an exposure of 7.25×10^{20} protons-on-target (POT). For this data set, 2451 charged current muon neutrino events were predicted in the Far Detector fiducial volume, but 1986 events were observed [9]. Consequently, the atmospheric mass-squared difference was found to be $\Delta m^2 = 2.32_{-0.08}^{+0.12} \times 10^{-3} \text{eV}^2$, and the mixing angle parameter $\sin^2(2\theta) > 0.90$ (90% C.L.). Exotic neutrino models like neutrino decoherence and neutrino decay were excluded at the 9σ and 7σ level respectively.

4. Muon Antineutrino Disappearance

MINOS has taken some data in antineutrino (reversed horn current) mode and carried out an antineutrino disappearance analysis [10]. For an exposure of 1.71×10^{20} POT, MINOS predicted 156 charged current $\bar{\nu}_\mu$ events in the absence of oscillations, however, 97 events were observed, thus disfavouring the no oscillations hypothesis at the 6.3σ level. The best fit antineutrino

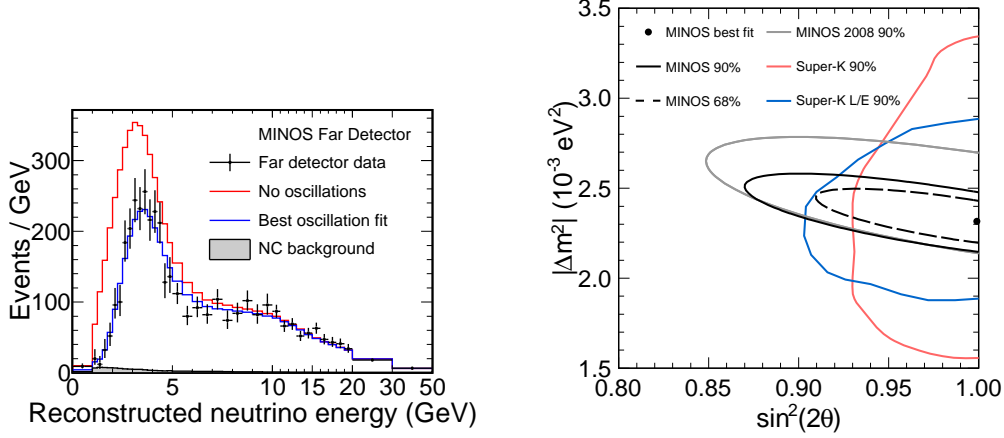


Figure 1: The left plot shows the energy spectrum of fully reconstructed Far Detector events classified as charged current interactions in black. The red histogram represents the spectrum predicted from measurements in the Near Detector assuming no oscillations, while the blue histogram reflects the best fit of the oscillation hypothesis. The shaded area shows the predicted neutral current background. The right plot shows the likelihood contours of 68% and 90% C.L. around the best fit values for the mass splitting and mixing angle. Also shown are contours from previous measurements [2, 3].

oscillation parameters were found to be $|\Delta\bar{m}^2| = (3.36_{-0.40}^{+0.46}(\text{stat.}) \pm 0.06(\text{syst.})) \times 10^{-3} \text{ eV}^2$ and $\sin^2(2\bar{\theta}) = 0.86_{-0.12}^{+0.11}(\text{stat.}) \pm 0.01(\text{syst.})$.

5. Electron Neutrino Appearance Analysis

Muon neutrinos may oscillate into electron neutrinos as they travel from the Near to the Far Detector. The corresponding oscillation probability is to first order given by:

$$P(\nu_\mu \rightarrow \nu_e) \approx \sin^2(2\theta_{13}) \sin^2 \theta_{23} \sin^2(1.27 \Delta m_{atm}^2 (L/E)) \quad (5.1)$$

If the oscillation angle θ_{13} is non-zero, then this should manifest itself as ν_e appearance at the Far Detector. In the case of MINOS, the search for ν_e appearance [11] is however made very difficult by low statistics and by a large background of neutral current events that mimic charged current ν_e events. To disentangle any potential signal from the large backgrounds, a number of cuts are applied to the data. First, a number of data quality cuts like timing and fiducial cuts are applied to select good beam events. Then, since ν_e -like events consist of electromagnetic showers, any events with long muon tracks are removed from the sample. Only events with at least one shower and a well-defined shower core, and within an energy range of 1-8 GeV, are selected for the final sample. Finally a selection algorithm is used to obtain the final data sample. This selection algorithm uses a MC library of 20 million signal and 30 million neutral current events to find the 50 best matches for each event and to construct three variables that are combined into a neural network to obtain a final discriminant variable (LEM).

In order to use the Near Detector data to predict the Far Detector data, the former is decomposed into its components: 60% neutral current events, 29% short-track charged current ν_μ events, and 11% intrinsic beam charged current ν_e events after all selection cuts. Those components are then extrapolated to the Far Detector using Monte Carlo Far/Near ratios accounting for various systematic errors such as flux, cross-section, fiducial volume, energy smearing, detector effects, and muon neutrino oscillation parameters. A ν_τ appearance component resultant from oscillated ν_μ is also added to the Far Detector prediction.

For the final analysis, MINOS uses five bins in reconstructed energy and three bins for the LEM discriminant variable (0.6-0.7, 0.7-0.8, and above 0.8). Systematic uncertainties taken into account include the composition of the Near Detector spectrum, the calibration (relative energy calibration, gains, absolute energy calibration), the relative Near/Far normalization, the hadronization model and other smaller uncertainties. In a signal enhanced region where $\text{LEM} > 0.7$, MINOS predicts $49.6 \pm 7.0(\text{stat.}) \pm 2.7(\text{syst.})$ events in the Far Detector for an exposure of 8.2×10^{20} , and observes 62 events. The final Far Detector spectra can be seen in Figure 2. If the final data are fitted to a neutrino appearance oscillation hypothesis, for a CP-violating phase $\delta=0$, MINOS finds $\sin^2 2\theta_{13} < 0.12$ for the normal mass hierarchy, and $\sin^2 2\theta_{13} < 0.20$ for the inverted mass hierarchy at the 90% C.L.. The corresponding best fit values are $\sin^2 2\theta_{13}=0.041$ for the normal mass hierarchy, and $\sin^2 2\theta_{13}=0.079$ for the inverted mass hierarchy. Figure 3 shows the final ν_e appearance limits obtained by MINOS. It can be seen that MINOS was able to exclude parameter space below the limit set by the Chooz experiment [12] for all values of δ for the normal mass hierarchy.

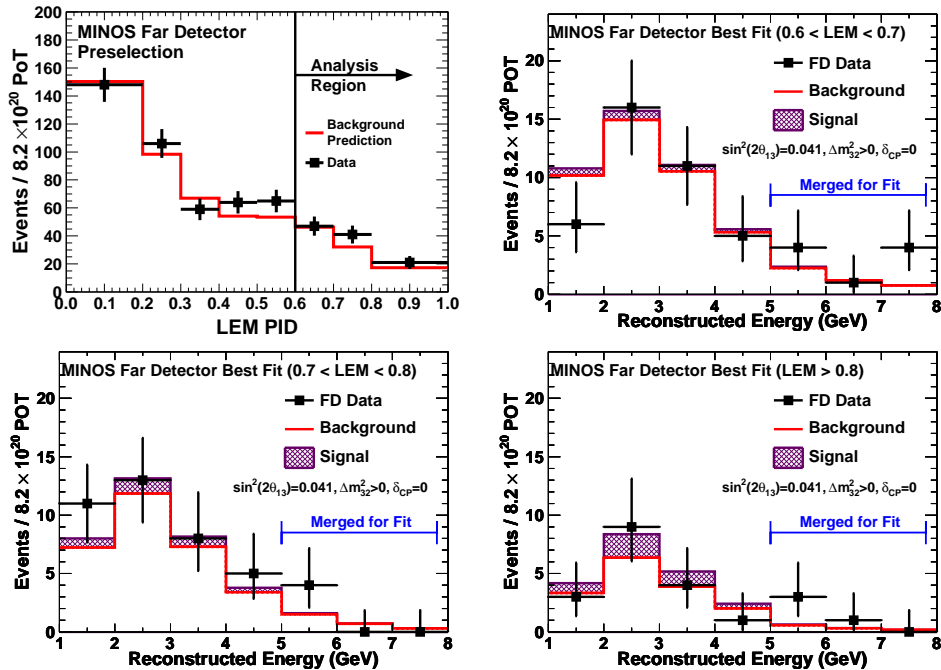


Figure 2: The top left plot shows the LEM discriminant variable distribution in the Far Detector. The top right plot and the bottom plots show the reconstructed energy spectra for charged current ν_e candidate events for the three LEM analysis bins. The black points show the data with statistical error bars. The red histograms show the expected background together with the contribution of ν_e appearance signal (hatched area) for the best-fit value of $\sin^2 2\theta_{13} = 0.041$.

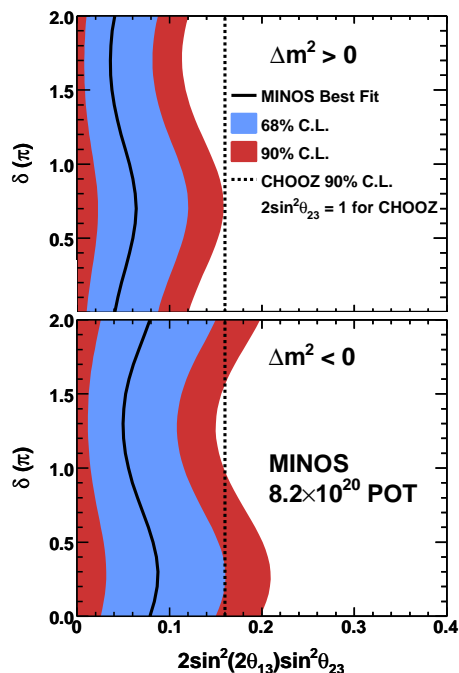


Figure 3: Allowed ranges and best fits for $2 \sin^2(2\theta_{13}) \sin^2 \theta_{23}$ as a function of CP-violating phase δ . The upper panel assumes the normal neutrino mass hierarchy, and the lower panel assumes the inverted mass hierarchy. The vertical dashed line shows the Chooz 90% C.L. upper limit assuming $\theta_{23}=45^\circ$ and $\Delta m_{32}^2=2.32 \text{ eV}^2$.

6. Conclusions

The MINOS experiment has carried out a number of analyses that are helping to measure and hone in on the values of the neutrino oscillation parameters. In the atmospheric sector, MINOS has been able to carry out the world's most precise measurement of the oscillation parameter Δm_{32}^2 . For the electron neutrino appearance analysis, MINOS has been able to set the world's tightest limit on $2 \sin^2(2\theta_{13}) \sin^2 \theta_{23}$ for the normal mass hierarchy.

This work was supported by the U.S. DOE; the U.K. STFC; the U.S. NSF; the State and University of Minnesota; the University of Athens, Greece; and Brazil's FAPESP, CNPq, and CAPES. We are grateful to the Minnesota Department of Natural Resources, the crew of the Soudan Underground Laboratory, and the staff of Fermilab for their contributions to this effort.

References

- [1] B. Pontecorvo, JETP 34, 172 (1958); V. N. Gribov and B. Pontecorvo, Phys. Lett. B28, 493 (1969); Z. Maki, M. Nakagawa, and S. Sakata, Prog. Theor. Phys. 28, 870 (1962).
- [2] Y. Ashie et al., Phys. Rev. Lett. 93, 101801 (2004); Y. Ashie et al., Phys. Rev. D71, 112005 (2005); J. Hosaka et al., Phys. Rev. D 74, 032002 (2006).
- [3] P. Adamson et al., Phys. Rev. Lett. 101, 131802 (2008).
- [4] B. Aharmim et al., Phys. Rev. C 72 055502 (2005).
- [5] S. Abe et al., Phys. Rev. Lett. 100, 221803 (2008).
- [6] M. H. Ahn et al., Phys. Rev. D 74, 072003 (2006).
- [7] P. Adamson et al., Phys. Rev. D 77 (2008).
- [8] D.G. Michael et al., Nucl.Inst.Meth. A 596 (2008).
- [9] P. Adamson et al., Phys. Rev. Lett. 106, 181801 (2011).
- [10] P. Adamson et al., Phys. Rev. Lett. 107, 021801 (2011).
- [11] P. Adamson et al., Phys. Rev. Lett. 107, 181802 (2011).
- [12] M. Apollonio et al., European Phys. Jour. C 27, 331 (2003).